1.6. Methods of space-group determination

U. Shmueli, H. D. Flack and J. C. H. Spence

1.6.1. Overview

This chapter describes and discusses several methods of symmetry determination of single-domain crystals. A detailed presentation of symmetry determination from diffraction data is given in Section 1.6.2.1, followed by a brief discussion of intensity statistics, ideal as well as non-ideal, with an application of the latter to real intensity data from a $P\overline{1}$ crystal structure in Section 1.6.2.2. Several methods of retrieving symmetry information from a solved crystal structure are then discussed (Section 1.6.2.3). This is followed by a discussion of chemical and physical restrictions on space-group symmetry (Section 1.6.2.4), including some aids in symmetry determination, and by a brief section on pitfalls in space-group determination (Section 1.6.2.5).

The following two sections deal with reflection conditions. Section 1.6.3 presents the theoretical background of conditions for possible general reflections and their corresponding derivation. A brief discussion of special reflection conditions is included. Section 1.6.4 presents an extensive tabulation of general reflection conditions and possible space groups.

Other methods of space-group determination are presented in Section 1.6.5. Section 1.6.5.1 deals with an account of methods of space-group determination based on resonant (also termed 'anomalous') scattering. Section 1.6.5.2 is a brief description of approaches to space-group determination in macromolecular crystallography. Section 1.6.5.3 deals with corresponding approaches in powder-diffraction methods.

The chapter concludes with a description and illustration of symmetry determination based on electron-diffraction methods (Section 1.6.6), and principally focuses on convergent-beam electron diffraction.

This chapter deals only with single crystals. A supplement (Flack, 2015) deals with twinned crystals and those displaying a specialized metric.

1.6.2. Symmetry determination from single-crystal studies

By U. Shmueli and H. D. Flack

1.6.2.1. Symmetry information from the diffraction pattern

The extraction of symmetry information from the diffraction pattern takes place in three stages.

In the first stage, the unit-cell dimensions are determined and analyzed in order to establish to which Bravais lattice the crystal belongs. A conventional choice of lattice basis (coordinate system) may then be chosen. The determination of the Bravais lattice[1] of the crystal is achieved by the process of cell reduction, in which the lattice is first described by a basis leading to a primitive unit cell, and then linear combinations of the unit-cell vectors are taken to reduce the metric tensor (and the cell dimensions) to a standard form. From the relationships amongst the elements of the metric tensor, one obtains the Bravais lattice, together with a conventional choice of the unit cell, with the aid of standard tables. A detailed description of cell reduction is given in Chapter 3.1 of this volume and in Part 9 of earlier editions (*e.g.* Burzlaff *et al.*, 2002). An alternative approach (Le Page, 1982) seeks the Bravais lattice directly from the cell dimensions by searching for all the twofold axes present. All these operations are automated in software. Regardless of the technique employed, at the end of the process one obtains an indication of the Bravais lattice and a unit cell in a conventional setting for the crystal system, primitive or centred as appropriate. These are usually good indications which, however, must be confirmed by an examination of the distribution of diffracted intensities as outlined below.

In the second stage, it is the point-group symmetry of the intensities of the Bragg reflections which is determined. We recall that the average reduced intensity of a pair of Friedel opposites (hkl and $\overline{hkl}$) is given by

$$\begin{aligned}|F_{\rm av}(\mathbf{h})|^2 &= \tfrac{1}{2}[|F(\mathbf{h})|^2 + |F(\overline{\mathbf{h}})|^2] \\ &= \sum_{i,j}[(f_i + f_i')(f_j + f_j') + f_i'' f_j'']\cos[2\pi\mathbf{h}(\mathbf{r}_i - \mathbf{r}_j)] \equiv A(\mathbf{h}),\end{aligned} \tag{1.6.2.1}$$

where the atomic scattering factor of atom j, taking into account resonant scattering, is given by

$$\mathbf{f}_j = f_j + f_j' + if_j'',$$

the wavelength-dependent components f_j' and f_j'' being the real and imaginary parts, respectively, of the contribution of atom j to the resonant scattering, $\mathbf{h}$ contains in the (row) matrix (1×3) the diffraction orders (hkl) and $\mathbf{r}_j$ contains in the (column) matrix (3×1) the coordinates (x_j, y_j, z_j) of atom j. The components of the $\mathbf{f}_j$ are assumed to contain implicitly the displacement parameters. Equation (1.6.2.1) can be found *e.g.* in Okaya & Pepinsky (1955), Rossmann & Arnold (2001) and Flack & Shmueli (2007). It follows from (1.6.2.1) that

$$|F_{\rm av}(\mathbf{h})|^2 = |F_{\rm av}(\overline{\mathbf{h}})|^2 \text{ or } A(\mathbf{h}) = A(\overline{\mathbf{h}}),$$

regardless of the contribution of resonant scattering. Hence the averaging introduces a centre of symmetry in the (averaged) diffraction pattern.[2] In fact, working with the average of Friedel opposites, one may determine the Laue group of the diffraction pattern by comparing the intensities of reflections which should be symmetry equivalent under each of the Laue groups. These are the 11 centrosymmetric point groups: $\overline{1}$, $2/m$, mmm, $4/m$, $4/mmm$, $\overline{3}$, $\overline{3}m$, $6/m$, $6/mmm$, $m\overline{3}$ and $m\overline{3}m$. For example, the reflections of which the intensities are to be compared for the Laue group $\overline{3}$ are: hkl, kil, ihl, $\overline{hkl}$, $\overline{kil}$ and $\overline{ihl}$, where $i = -h - k$. An extensive listing of the indices of symmetry-related reflections in all the point groups, including of course the Laue groups, is

[1] The Bravais lattice symbol consists of two characters. The first is the first letter of the name of a crystal family and the second is the centring mode of a conventional unit cell. For details see Tables 3.1.2.1 and 3.1.2.2.

[2] We must mention the well known Friedel's law, which states that $|F(\mathbf{h})|^2 = |F(\overline{\mathbf{h}})|^2$ and which is only a reasonable approximation for noncentrosymmetric crystals if resonant scattering is negligibly small. This law holds well for centrosymmetric crystals, independently of the resonant-scattering contribution.

given in Appendix 1.4.4 of *International Tables for Crystallography* Volume B (Shmueli, 2008).[3] In the past, one used to inspect the diffraction images to see which classes of reflections are symmetry equivalent within experimental and other uncertainty. Nowadays, the whole intensity data set is analyzed by software. The intensities are merged and averaged under each of the 11 Laue groups in various settings (*e.g.* 2/*m* unique axis *b* and unique axis *c*) and orientations (*e.g.* $\bar{3}m1$ and $\bar{3}1m$). For each choice of Laue group and its variant, an $R_{\rm merge}$ factor is calculated as follows:

$$R_{{\rm merge},i} = \frac{\sum_{\mathbf{h}} \sum_{s=1}^{|G|_i} |\langle |F_{\rm av}(\mathbf{h})|^2 \rangle_i - |F_{\rm av}(\mathbf{h}\boldsymbol{W}_{si})|^2|}{|G|_i \sum_{\mathbf{h}} \langle |F_{\rm av}(\mathbf{h})|^2 \rangle_i}, \qquad (1.6.2.2)$$

where $\boldsymbol{W}_{si}$ is the matrix of the *s*th symmetry operation of the *i*th Laue group, $|G_i|$ is the number of symmetry operations in that group, the average in the first term in the numerator and in the denominator ranges over the intensities of the trial Laue group and the outer summations $\sum_{\mathbf{h}}$ range over the *hkl* reflections. Choices with low $R_{{\rm merge},i}$ display the chosen symmetry, whereas for those with high $R_{{\rm merge},i}$ the symmetry is inappropriate. The Laue group of highest symmetry with a low $R_{{\rm merge},i}$ is considered the best indication of the Laue group. Several variants of the above procedure exist in the available software. Whichever of them is used, it is important for the discrimination of the averaging process to choose a strategy of data collection such that the intensities of the greatest possible number of Bragg reflections are measured. In practice, validation of symmetry can often be carried out with a few initial images and the data-collection strategy may be based on this assignment.

In the third stage, the intensities of the Bragg reflections are studied to identify the conditions for systematic absences. Some space groups give rise to zero intensity for certain classes of reflections. These 'zeros' occur in a systematic manner and are commonly called systematic absences (*e.g.* in the *h*0*l* class of reflections, if all rows with *l* odd are absent, then the corresponding reflection condition is *h*0*l*: $l = 2n$). In practice, as implemented in software, statistics are produced on the intensity observations of all possible sets of 'reflections conditions' as given in Chapter 2.3 (*e.g.* in the example above, *h*0*l* reflections are separated into sets with $l = 2n$ and those with $l = 2n + 1$). In one approach, the number of observations in each set having an intensity (I) greater than n standard uncertainties [$u(I)$] [*i.e.* $I/u(I) > n$] is displayed for various values of n. Clearly, if a trial condition for systematic absence has observations with strong or medium intensity [*i.e.* $I/u(I) > 3$], the systematic-absence condition is not fulfilled (*i.e.* the reflections are not systematically absent). If there are no such observations, the condition for systematic absence may be valid and the statistics for smaller values of n need then to be examined. These are more problematic to evaluate, as the set of reflections under examination may have many weak reflections due to structural effects of the crystal or to perturbations of the measurements by other systematic effects. An alternative approach to examining numbers of observations is to compare the mean value, $\langle I/u(I) \rangle$, taken over reflections obeying or not a trial reflection condition. For a valid reflection condition, one expects the former value to be considerably larger than the latter. In Section 3.1 of Palatinus & van der Lee (2008), real examples of marginal cases are described.

[3] The tables in Appendix 1.4.4 mentioned above actually deal with space groups in reciprocal space; however, the left part of any entry is just the indices of a reflection generated by the point-group operation corresponding to this entry.

Table 1.6.2.1
The ability of the procedures described in Sections 1.6.2.1 and 1.6.5.1 to distinguish between space groups

The columns of the table show the number of sets of space groups that are indistinguishable by the chosen technique, according to the number of space groups in the set, *e.g.* for Laue-class discrimination, 85 space groups may be uniquely identified, whereas there are 8 sets containing 5 space groups indistinguishable by this technique. The tables in Section 1.6.4 contain 416 different settings of space groups generated from the 230 space-group types.

	No. of space groups in set that are indistinguishable by procedure used					
	1	2	3	4	5	6
No. of sets for Laue-class discrimination	85	78	43	0	8	1
No. of sets for point-group discrimination	390	13	0	0	0	0

The third stage continues by noting that the systematic absences are characteristic of the space group of the crystal, although some sets of space groups have identical reflection conditions. In Chapter 2.3 one finds all the reflection conditions listed individually for the 230 space groups. For practical use in space-group determination, tables have been set up that present a list of all those space groups that are characterized by a given set of reflection conditions. The tables for all the Bravais lattices and Laue groups are given in Section 1.6.4 of this chapter. So, once the reflection conditions have been determined, all compatible space groups can be identified from the tables. Table 1.6.2.1 shows that 85 space groups may be unequivocally determined by the procedures defined in this section based on the identification of the Laue group. For other sets of reflection conditions, there are a larger number of compatible space groups, attaining the value of 6 in one case. It is appropriate at this point to anticipate the results presented in Section 1.6.5.1, which exploit the resonant-scattering contribution to the diffracted intensities and under appropriate conditions allow not only the Laue group but also the point group of the crystal to be identified. If such is the case, the last line of Table 1.6.2.1 shows that almost all space groups can be unequivocally determined. In the remaining 13 pairs of space groups, constituting 26 space groups in all, there are the 11 enantiomorphic pairs of space groups [($P4_1$–$P4_3$), ($P4_122$–$P4_322$), ($P4_12_12$–$P4_32_12$), ($P3_1$–$P3_2$), ($P3_121$–$P3_221$), ($P3_112$–$P3_212$), ($P6_1$–$P6_5$), ($P6_2$–$P6_4$), ($P6_122$–$P6_522$), ($P6_222$–$P6_422$) and ($P4_132$–$P4_332$)] and the two exceptional pairs of $I222$ & $I2_12_12_1$ and $I23$ & $I2_13$, characterized by having the same symmetry elements in a different arrangement in space. These 13 pairs of space groups cannot be distinguished by the methods described in Sections 1.6.2 and 1.6.5.1, but may be distinguished when a reliable atomic structural model of the crystal has been obtained. On the other hand, all these 13 pairs of space groups can be distinguished by the methods described in Section 1.6.6 and in detail in Saitoh *et al.* (2001). It should be pointed out in connection with this third stage that a possible weakness of the analysis of systematic absences for crystals with small unit-cell dimensions is that there may be a small number of axial reflections capable of being systematically absent.

It goes without saying that the selected space groups must be compatible with the Bravais lattice determined in stage 1, with the Laue class determined in stage 2 and with the set of space-group absences determined in stage 3.

We thank L. Palatinus (2011) for having drawn our attention to the unexploited potential of the Patterson function for the determination of the space group of the crystal. The discovery of

this method is due to Buerger (1946) and later obtained only a one-sentence reference by Rogers (1950) and by Rossmann & Arnold (2001). The method is based on the observation that interatomic vectors between symmetry-related (other than by inversion in a point) atoms cause peaks to accumulate in the corresponding Harker sections and lines of the Patterson function. It is thus only necessary to find the location of those Harker sections and lines that have a high concentration of peaks to identify the corresponding symmetry operations of the space group. At the time of its discovery, it was not considered an economic method of space-group determination due to the labour involved in calculating the Patterson function. Subsequently it was completely neglected and there are no recent reports of its use. It is thus not possible to report on its strengths and weaknesses in practical modern-day applications.

1.6.2.2. Structure-factor statistics and crystal symmetry

Most structure-solving software packages contain a section dedicated to several probabilistic methods based on the Wilson (1949) paper on the probability distribution of structure-factor magnitudes. These statistics sometimes correctly indicate whether the intensity data set was collected from a centrosymmetric or noncentrosymmetric crystal. However, not infrequently these indications are erroneous. The reasons for this may be many, but outstandingly important are (i) the presence of a few very heavy atoms amongst a host of lighter ones, and (ii) a very small number of nearly equal atoms. Omission of weak reflections from the data set also contributes to failures of Wilson (1949) statistics. These erroneous indications are also rather strongly space-group dependent.

The well known probability density functions (hereafter p.d.f.'s) of the magnitude of the normalized structure factor E, also known as ideal p.d.f.'s, are

$$p(|E|) = \begin{cases} \sqrt{2/\pi}\exp\left(-|E|^2/2\right) & \text{for } P\overline{1} \\ 2|E|\exp(-|E|^2) & \text{for } P1 \end{cases}, \qquad (1.6.2.3)$$

where it is assumed that all the atoms are of the same chemical element. Let us see their graphical representations.

It is seen from Fig. 1.6.2.1 that the two p.d.f.'s are significantly different, but usually they are not presented as such by the software. What is usually shown are the cumulative distributions of $|E|^2$, the moments: $\langle|E|^n\rangle$ for $n = 1, 2, 3, 4, 5, 6$, and the averages of low powers of $|E^2 - 1|$ for ideal centric and acentric distributions, based on equation (1.6.2.3). Table 1.6.2.2 shows the numerical values of several low-order moments of $|E|$ and that of the lowest power of $|E^2 - 1|$. The higher the value of n the greater is the difference between their values for centric and acentric cases. However, it is most important to remember that the influence of measurement uncertainties also increases with n and therefore the higher the moment the less reliable it tends to be.

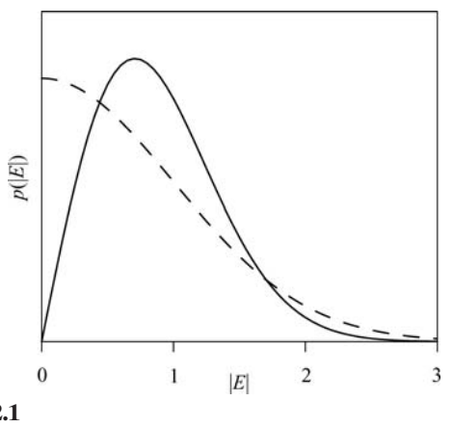

Figure 1.6.2.1
Ideal p.d.f.'s for the equal-atom case. The dashed line is the centric, and the solid line the acentric ideal p.d.f.

Table 1.6.2.2
The numerical values of several low-order moments of $|E|$, based on equation (1.6.2.3)

Moment	$P\overline{1}$	$P1$
$\langle\|E\|\rangle$	0.798	0.886
$\langle\|E\|^2\rangle$	1.000	1.000
$\langle\|E\|^3\rangle$	1.596	1.329
$\langle\|E\|^4\rangle$	3.000	2.000
$\langle\|E\|^5\rangle$	6.383	3.323
$\langle\|E\|^6\rangle$	15.000	6.000
$\langle\|E^2 - 1\|\rangle$	0.968	0.736

There are several ideal indicators of the status of centrosymmetry of a crystal structure. The most frequently used are: (i) the $N(z)$ test (Howells *et al.*, 1950), a cumulative distribution of $z = |E|^2$, based on equation (1.6.2.3), and (ii) the low-order moments of $|E|$, also based on equation (1.6.2.3). Equation (1.6.2.3), however, is very seldom used as an indicator of the status of centrosymmetry of a crystal stucture.

Let us now briefly consider p.d.f.'s that are valid for any atomic composition as well as any space-group symmetry, and exemplify their performance by comparing a histogram derived from observed intensities from a $P\overline{1}$ structure with theoretical p.d.f.'s for the space groups $P1$ and $P\overline{1}$. The p.d.f.'s considered presume that all the atoms are in general positions and that the reflections considered are general (see, *e.g.*, Section 1.6.3). A general treatment of the problem is given in the literature and summarized in the book *Introduction to Crystallographic Statistics* (Shmueli & Weiss, 1995).

The basics of the exact p.d.f.'s are conveniently illustrated in the following. The normalized structure factor for the space group $P\overline{1}$, assuming that all the atoms occupy general positions and resonant scattering is neglected, is given by

$$E(\mathbf{h}) = 2\sum_{j=1}^{N/2} n_j \cos(2\pi\mathbf{h}\boldsymbol{r}_j),$$

where n_j is the normalized scattering factor. The maximum possible value of E is $E_{\max} = \sum_{j=1}^{N} n_j$ and the minimum possible value of E is $-E_{\max}$. Therefore, $E(\mathbf{h})$ must be confined to the $(-E_{\max}, E_{\max})$ range. The probability of finding E outside this range is of course zero. Such a probability density function can be expanded in a Fourier series within this range (*cf.* Shmueli *et al.*, 1984). This is the basis of the derivation, the details of which are well documented (*e.g.* Shmueli *et al.*, 1984; Shmueli & Weiss, 1995; Shmueli, 2007). Exact p.d.f.'s for any centrosymmetric space group have the form

$$p(|E|) = \alpha\left\{1 + 2\sum_{m=1}^{\infty} C_m \cos(\pi m|E|\alpha)\right\}, \qquad (1.6.2.4)$$

where $\alpha = 1/E_{\max}$, and exact p.d.f.'s for any noncentrosymmetric space group can be computed as the double Fourier series

$$p(|E|) = \tfrac{1}{2}\pi\alpha^2|E|\sum_{m=1}^{\infty}\sum_{n=1}^{\infty} C_{mn} J_0[\pi\alpha|E|(m^2 + n^2)^{1/2}], \qquad (1.6.2.5)$$

where $J_0(X)$ is a Bessel function of the first kind and of order zero. Expressions for the coefficients C_m and C_{mn} are given by

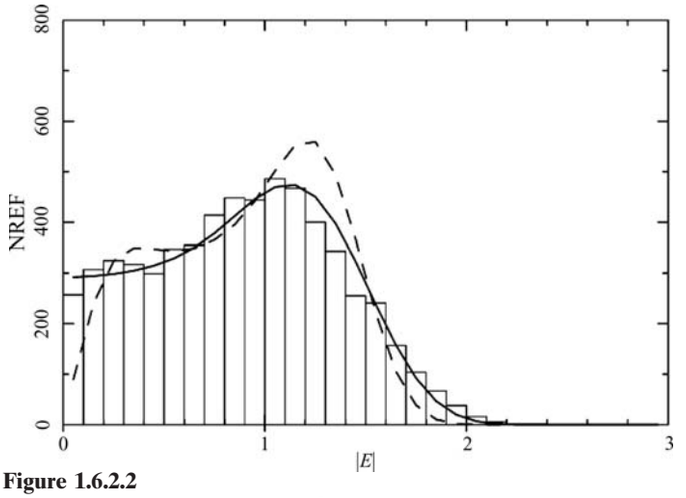

Figure 1.6.2.2
Exact p.d.f.'s. for a crystal of [(*Z*)-ethyl *N*-isopropylthiocarbamato-κS](tricyclohexylphosphine-κP)gold(I) in the triclinic system. Solid curve: $P\overline{1}$, computed from (1.6.2.4); dashed curve: *P*1, computed from (1.6.2.5); histogram based on the data computed from all the reflections with non-negative reduced intensities. The height of each bin corresponds to the number of reflections (NREF) in its range of $|E|$ values. The p.d.f.'s are scaled up to the histogram.

Rabinovich *et al.* (1991) and by Shmueli & Wilson (2008) for all the space groups up to and including $Fd\overline{3}$.

The following example deals with a very high sensitivity to atomic heterogeneity. Consider the crystal structure of [(*Z*)-ethyl *N*-isopropylthiocarbamato-κS](tricyclohexylphosphine-κP)gold(I), published as $P\overline{1}$ with $Z = 2$, the content of its asymmetric unit being $AuSPONC_{24}H_{45}$ (Tadbuppa & Tiekink, 2010). Let us construct a histogram from the $|E|$ data computed from all the observed reflections with non-negative reduced intensities and compare the histogram with the p.d.f.'s for the space groups *P*1 and $P\overline{1}$, computed from equations (1.6.2.5) and (1.6.2.4), respectively. The histogram and the p.d.f.'s were put on the same scale. The result is shown in Fig. 1.6.2.2.

A visual comparison strongly indicates that the space-group assignment as $P\overline{1}$ was correct, since the recalculated histogram agrees rather well with the p.d.f. (1.6.2.4) and much less with (1.6.2.5). The ideal Wilson-type statistics incorrectly indicated that this crystal is noncentrosymmetric. It is seen that the ideal p.d.f. breaks down in the presence of strong atomic heterogeneity (gold among many lighter atoms) in the space group $P\overline{1}$. Other space groups behave differently, as shown in the literature (*e.g.* Rabinovich *et al.*, 1991; Shmueli & Weiss, 1995).

Additional examples of applications of structure-factor statistics and some relevant computing considerations and software can be found in Shmueli (2012) and Shmueli (2013).

1.6.2.3. Symmetry information from the structure solution

It is also possible to obtain information on the symmetry of the crystal after structure solution. The latter is obtained either in space group *P*1 (*i.e.* no symmetry assumed) or in some other candidate space group. The analysis may take place either on the electron-density map, or on its interpretation in terms of atomic coordinates and atomic types (*i.e.* chemical elements). The analysis of the electron-density map has become increasingly popular with the advent of dual-space methods, first proposed in the charge-flipping algorithm by Oszlányi & Sütő (2004), which solve structures in *P*1 by default. The analysis of the atomic coordinates and atomic types obtained from least-squares refinement in a candidate space group is used extensively in structure validation. Symmetry operations present in the structure solution but not in the candidate space group are sought.

An exhaustive search for symmetry operations is undertaken. However, those to be investigated may be very efficently limited by making use of knowledge of the highest point-group symmetry of the lattice compatible with the known cell dimensions of the crystal. It is well established that the point-group symmetry of any lattice is one of the following seven centrosymmetric point groups: $\overline{1}$, 2/*m*, *mmm*, 4/*mmm*, $\overline{3}m$, 6/*mmm*, $m\overline{3}m$. This point group is known as the holohedry of the lattice. The relationship between the symmetry operations of the space group and its holohedry is rather simple. A rotation or screw axis of symmetry in the crystal has as its counterpart a corresponding rotation axis of symmetry of the lattice and a mirror or glide plane in the crystal has as its counterpart a corresponding mirror plane in the lattice. The holohedry may be equal to or higher than the point group of the crystal. Hence, at least the rotational part of any space-group operation should have its counterpart in the symmetry of the lattice. If and when this rotational part is found by a systematic comparison either of the electron density or of the positions of the independent atoms of the solved structure, the location and intrinsic parts of the translation parts of the space-group operation can be easily completed.

Palatinus and van der Lee (2008) describe their procedure in detail with useful examples. It uses the structure solution both in the form of an electron-density map and a set of phased structure factors obtained by Fourier transformation. No interpretation of the electron-density map in the form of atomic coordinates and chemical-element type is required. The algorithm of the procedure proceeds in the following steps:

(1) The lattice centring is determined by a search for strong peaks in the autocorrelation (self-convolution, Patterson) function of the electron density and the potential centring vectors are evaluated through a reciprocal-space *R* value.
(2) A complete list of possible symmetry operations compatible with the lattice is generated by searching for the invariance of the direct-space metric under potential symmetry operations.
(3) A figure of merit is then assigned to each symmetry operation evaluated from the convolution of the symmetry-transformed electron density with that of the structure solution. Those symmetry operations that have a good figure of merit are selected as belonging to the space group of the crystal structure.
(4) The space group is completed by group multiplication of the selected operations and then validated.
(5) The positions of the symmetry elements are shifted to those of a conventional setting for the space group.

Palatinus & van der Lee (2008) report a very high success rate in the use of this algorithm. It is also a powerful technique to apply in structure validation.

Le Page's (1987) pioneering software *MISSYM* for the detection of 'missed' symmetry operations uses refined atomic coordinates, unit-cell dimensions and space group assigned from the crystal-structure solution. The algorithm follows all the principles described above in this section. In *MISSYM*, the metric symmetry is established as described in the first stage of Section 1.6.2.1. The 'missed' symmetry operations are those that are present in the arrangement of the atoms but are not part of the space group used for the structure refinement. Indeed, this procedure has its main applications in structure validation. The algorithm used in Le Page's software is also implemented in *ADDSYM* (Spek, 2003). There are numerous reports of successful applications of this software in the literature.

1.6.2.4. Restrictions on space groups

The values of certain chemical and physical properties of a bulk compound, or its crystals, have implications for the assignment of the space group of a crystal structure. In the chemical domain, notably in proteins and small-molecule natural products, information concerning the enantiomeric purity of the bulk compound or of its individual crystals is most useful. Further, all physical properties of a crystal are limited by the point group of the crystal structure in ways that depend on the individual nature of the physical property.

It is very well established that the crystal structure of an enantiomerically pure compound will be chiral (see Flack, 2003). By an enantiomerically pure compound one means a compound whose molecules are all chiral and all these molecules possess the same chirality. The space group of a chiral crystal structure will only contain the following types of symmetry operation: translations, pure rotations and screw rotations. Inversion in a point, mirror reflection or rotoinversion do not occur in the space group of a chiral crystal structure. Taking all this together means that the crystal structure of an enantiomerically pure compound will show one of 65 space groups (known as the Sohncke space groups), all noncentrosymmetric, containing only translations, rotations and screw rotations. As a consequence, the point group of a chiral crystal structure is limited to the 11 point groups containing only pure rotations (*i.e.* 1, 2, 222, 4, 422, 3, 32, 6, 622, 23 and 432). Particular attention must be paid as to whether a measurement of enantiomeric purity of a compound applies to the bulk material or to the single crystal used for the diffraction experiment. Clearly, a compound whose bulk is enantiomerically pure will produce crystals which are enantiomerically pure. The converse is not necessarily true (*i.e.* enantiomerically pure crystals do not necessarily come from an enantiomerically pure bulk). For example, a bulk compound which is a racemate (*i.e.* an enantiomeric mixture containing 50% each of the opposite enantiomers) may produce either (*a*) crystals of the racemic compound (*i.e.* crystals containing 50% each of the opposite enantiomers) or (*b*) a racemic conglomerate (*i.e.* a mixture of enantiomerically pure crystals in a proportion of 50% of each pure enantiomer) or (*c*) some other rarer crystallization modes. Consequently, as part of a single-crystal structure analysis, it is highly recommended to make a measurement of the enantiomeric purity of the single crystal used for the diffraction experiment.

Much information on methods of establishing the enantiomeric purity of a compound can be found in a special issue of *Chirality* devoted to the determination of absolute configuration (Allenmark *et al.*, 2007). Measurements in the fluid state of optical activity, optical rotatory dispersion (ORD), circular dichroism (CD) and enantioselective chromatography are of prime importance. Many of these are sufficiently sensitive to be applicable not only to the bulk compound but also to the single crystal used for the diffraction experiment taken into solution. CD may also be applied in the solid state.

Many physical properties of a crystalline solid are anisotropic and the symmetry of a physical property of a crystal is limited both by the point-group symmetry of the crystal and by symmetries inherent to the physical property under study. For further information on this topic see Part 1 of Volume D (Authier *et al.*, 2014). Unfortunately, many of these physical properties are intrinsically centrosymmetric, so few of them are of use in distinguishing between the subgroups of a Laue group, a common problem in space-group determination. In Chapter 3.2 of the present volume, Hahn & Klapper show to which point groups a crystal must belong to be capable of displaying some of the principal physical properties of crystals (Table 3.2.2.1). Measurement of morphology, pyroelectricity, piezoelectricity, second harmonic generation and optical activity of a crystalline sample can be of use.

1.6.2.5. Pitfalls in space-group determination

The methods described in Sections 1.6.2 and 1.6.5.1 rely on the crystal measured being a single-domain crystal, *i.e.* it should not be twinned. Nevertheless, some types of twin are easily identified at the measurement stage as they give rise to split reflections. Powerful data-reduction techniques may be applied to data from such crystals to produce a reasonably complete single-domain intensity data set. Consequently, the multi-domain twinned crystals that give rise to difficulties in space-group determination are those for which the reciprocal lattices of the individual domains overlap exactly without generating any splitting of the Bragg reflections. A study of the intensity data from such a crystal may display two anomalies. Firstly, the intensity distribution, as described and analysed in Section 1.6.2.2, will be broader than that of the monodomain crystal. Secondly, one may obtain a set of conditions for reflections that does not correspond to any entry in Section 1.6.4. In this chapter we give no further information on the determination of the space group for such twinned crystals. For further information on this topic see Part 3 of Volume D (Boček *et al.*, 2006) and Chapter 1.3 on twinning in Volume C (Koch, 2006). A supplement (Flack, 2015) to the current section deals with the determination of the space group from twinned crystals and those displaying a specialized metric. However, it is apposite to note that the existence of twins with overlapping reciprocal lattices can be identified by recording atomic resolution transmission electron-microscope images.

In order to obtain reliable results from space-group determination, the coverage of the reciprocal space by the intensity measurements should be as complete as possible. One should attempt to attain full-sphere data coverage, *i.e.* a complete set of intensity measurements in the point group 1. All Friedel opposites should be measured. The validity and reliability of the intensity statistics described in Section 1.6.2.2 rest on a full coverage of reciprocal lattice. Any systematic omission by resolution, azimuth and declination, intensity *etc.* of part of the asymmetric region of the reciprocal lattice has an adverse effect. In particular, reflections of weak intensity should not be omitted or deleted.

There are a few other common difficulties in space-group determination due either to the nature of the crystal or the experimental setup:

(*a*) The crystal may display a pseudo-periodicity leading to systematic series of weak or very weak reflections that can be mistaken for systematic absences.

(*b*) The physical effect of multiple reflections can lead to diffraction intensity appearing at the place of systematic absences. However, the shape of these multiple-reflection intensities is usually much sharper than a normal Bragg reflection.

(*c*) Contamination of the incident radiation by a $\lambda/2$ component may also cause intensity due to the $2h\,2k\,2l$ reflection to appear at the place of the hkl one. Kirschbaum *et al.* (1997) and Macchi *et al.* (1998) have studied this probem and describe ways of circumventing it.

references